Zeppelin-led study on the onset of new particle formation in the planetary boundary layer

Janne Lampilahti[1], Hanna E. Manninen[2], Tuomo Nieminen[1], Sander Mirme[3], Mikael Ehn[1], Iida Pullinen[4], Katri Leino[1], Siegfried Schobesberger[1,4], Juha Kangasluoma[1], Jenni Kontkanen[1], Emma Järvinen[5], Riikka Väänänen[1], Taina Yli-Juuti[4], Radovan Krejci[6], Katrianne Lehtipalo[1,7], Janne Levula[1], Aadu Mirme[3], Stefano Decesari[8], Ralf Tillmann[9], Douglas R. Worsnop[1,4,10], Franz Rohrer[9], Astrid Kiendler-Scharr[9], Tuukka Petäjä[1,11], Veli-Matti Kerminen[1], Thomas F. Mentel[9], and Markku Kulmala[1,11,12]

[1]Institute for Atmospheric and Earth System Research / Physics, Faculty of Science, University of Helsinki, Helsinki, Finland.
[2]CERN, CH-1211 Geneva, Switzerland.
[3]Institute of Physics, University of Tartu, Tartu, Estonia.
[4]Department of Applied Physics, University of Eastern Finland, Kuopio, Finland.
[5]National Center for Atmospheric Research, Boulder, CO, USA.
[6]Department of Environmental Science & Bolin Centre for Climate research, Stockholm University, Stockholm, Sweden.
[7]Finnish Meteorological Institute, Helsinki, Finland.
[8]Istituto di Scienze dell'Atmosfera e del Clima, CNR, Bologna, Italy.
[9]Institute for Energy and Climate Research, IEK-8, Forschungszentrum Jülich GmbH, Jülich, Germany.
[10]Aerodyne Research Inc, Billerica, MA, USA.
[11]Joint International Research Laboratory of Atmospheric and Earth System Sciences, Nanjing. University, Nanjing, China.
[12]Aerosol and Haze Laboratory, Beijing Advanced Innovation Center for Soft Matter Science and Engineering, Beijing University of Chemical Technology, Beijing, China.

Correspondence to: Janne Lampilahti (janne.lampilahti@helsinki.fi)

Abstract

We compared observations of aerosol particle formation and growth in different parts of the planetary boundary layer at two different environments that have frequent new particle formation (NPF) events. In summer 2012 we had a campaign in Po Valley, Italy (urban background) and in spring 2013 a similar campaign took place in Hyytiälä, Finland (rural background). Our study consists of three case studies of airborne and ground-based measurements of ion and particle size distribution from ~1 nm. The airborne measurements were performed using a Zeppelin inside the boundary layer up to 1000 m altitude. Our observations show the onset of regional NPF and the subsequent growth of the aerosol particles happening almost uniformly inside the mixed layer (ML) in both locations. However, in Hyytiälä we noticed local enhancement in the intensity of NPF caused by mesoscale BL dynamics. Additionally, our observations indicate that in Hyytiälä NPF was probably also taking place above the ML. In Po Valley we observed NPF that was limited to a specific air mass.

1 Introduction

The boundary layer (BL) is the lowest layer of the earth's atmosphere (Stull, 1988). The BL is an interface controlling the exchange of mass and energy between atmosphere and surface. Ground based measurements are often used as representative observations for the whole BL. However they cannot cover vertical internal variability of BL and this can be addressed only by airborne observations.

Figure 1 show the typical BL evolution over land during the time span on one day. Shortly after sunrise convective mixing creates a mixed layer (ML) that rapidly grows during the morning by entraining air from above and can reach an altitude of ~1-2 km above the surface. The ML is capped by a stable layer at the top. Above the BL is the free troposphere (FT), which is decoupled from the surface. Here we define BL to mean all the layers below the FT. Around sunset convective mixing and turbulence diminishes and the ML becomes what is known as the residual layer (RL). During the night a stable boundary layer develops due to interaction with the ground surface. This layer has only weak intermittent turbulence and it smoothly blends into the RL.

We studied where new particle formation (NPF) occurs in the BL and how it relates to BL evolution, comparing two different environments. NPF refers to the formation of nanometer sized clusters from low-volatility vapors present in the atmosphere, and their subsequent growth to larger aerosol particles (Kulmala et al., 2013). Understanding NPF better is of major interest, since it is a dominant source of cloud condensation nuclei in the atmosphere and therefore can have important indirect effects on climate (Dunne et al., 2016; Gordon et al., 2017; Pierce and Adams, 2009; Yu and Luo, 2009).

Nilsson et al. (2001) studied NPF in a boreal forest environment and observed that in addition to increased solar radiation the onset of turbulence appears to be a necessary trigger for NPF. Several explanations for this connection were proposed: NPF might be starting in the RL or at the top of the shallow ML, from where the aerosol particles are mixed to the surface as the ML starts to grow. NPF starts in the ML due to dilution of pre-existing aerosol and drop in vapor sink. Convective mixing brings different precursor gases, one present in the RL and the other in the ML, into contact with each other initiating NPF inside the ML.

Airborne measurements of nanoparticles from different environments show that NPF occurs in many parts of the BL. Multiple observations from Central Europe suggest that aerosol particles are formed on top of a shallow ML (Platis et al., 2015; Siebert et al., 2004; Chen et al., 2018) or inside the RL (Stratmann et al., 2003; Wehner et al., 2010). Other results come from a boreal forest environment in southern Finland. Lampilahti et al. (2021) showed evidence that NPF may occur in the interface between the RL and the FT. O'Dowd et al. (2009) observed the first signs of NPF in the surface ML and Leino et al. (2019) showed that sub-3 nm particles have higher concentration close to surface. Laakso et al. (2007) performed hot-air balloon measurements and concluded that NPF either took place throughout the ML or in the lower part of the ML. Measurements by Schobesberger et al. (2013) suggested that NPF was more intense in the top parts of a developed ML. More measurements are needed in order to understand these mixed results.

Here we present NPF measurements on board a Zeppelin airship carried out during the EU supported PEGASOS (Pan-European Gas-AeroSOls Climate Interaction Study) project. The Zeppelin flights were used to observe radicals, trace gases, and aerosol particles inside the lower troposphere over Europe in several locations during 2012-2013.

By using a Zeppelin NT (Neue Technologie) airship we were able to sample up to 1000 meters above sea level (asl). The high payload capacity of the Zeppelin enabled us to carry state-of-the-art instrumentation, specifically designed to collect information on the feedback processes between the chemical compounds and the smallest aerosol particles to better estimate their role in climate and air quality.

The NPF focused campaigns presented here were performed in Po Valley, Italy, and Hyytiälä, Finland. At both locations NPF events happen frequently. Po Valley represents urban background conditions where anthropogenic emissions are an important source of gaseous precursors for NPF (e.g. Kontkanen et al., 2016). Hyytiälä represents rural background conditions where organic vapors from the surrounding forests play a major role in NPF (e.g. Dada et al., 2017).

Here we combine comprehensive ground-based and airborne measurements from the Zeppelin to investigate two NPF cases from Po Valley and one case from Hyytiälä. The Zeppelin allowed us to repeatedly profile the lowest 1 km of the atmosphere providing a full picture of what is happening in the BL during the onset of NPF. We will show in which part or parts of the BL the onset of NPF and the subsequent particle growth occurred at the two measurement sites as well as determine formation and growth rates for the aerosol particles.

2 Methods

The two ground-based measurement sites that were studied here were San Pietro Capofiume in Po Valley, Italy and Hyytiälä in Southern Finland. The vertical measurement profiles analyzed in this study were performed in a close proximity to the ground-based measurement sites.

2.1 San Pietro Capofiume, Italy

San Pietro Capofiume (SPC, 44°39'N 11°37'E, 11 m asl) is located in the eastern part of Po Valley, Italy, between the cities of Bologna and Ferrara. Po Valley is considered a pollution hot spot, although, the station itself is surrounded by vast agricultural fields away from point sources. Thus the aerosol concentration and composition at SPC reflect the Po Valley regional background. NPF is frequently observed in SPC (36% of days) with maxima in May and July (Hamed et al., 2007; Laaksonen et al., 2005).

The instruments measuring the aerosol particle number-size distribution were a scanning mobility particle sizer (SMPS, 10-700 nm, 5 min time resolution; Wiedensohler et al., 2012) and a neutral cluster and air ion spectrometer (NAIS, particles: ~2-40 nm, ions: 0.8-40 nm, 4 min time resolution; Mirme and Mirme, 2013). We used the NAIS's positive polarity for the particle number size distribution data. The ML height was determined from ceilometer (Lufft CHM 15k) measurements. Basic meteorology and SO_2 gas concentration data (Thermo 43iTLE monitor) were also available at surface level (2-3 m above ground level).

2.2 Hyytiälä, Finland

In Finland the ground-based measurements were performed at the SMEAR II (Station for Measuring Forest Ecosystem-Atmosphere Relations II) station located in Hyytiälä, Finland (HTL, 61°51’N 24°17’E, 181 m asl; Hari and Kulmala, 2005). The station is equipped with extensive facilities to measure the forest ecosystem and the atmosphere. The measurement site is surrounded by coniferous boreal forest.

The forest emits biogenic volatile organic compounds (Hakola et al., 2003), which can be oxidized in the atmosphere to form low-volatile vapors that contribute to aerosol particle formation and growth (Ehn et al., 2014; Mohr et al., 2019). NPF is frequently observed in HTL (23% of all days), especially in spring and autumn (Dal Maso et al., 2005; Nieminen et al., 2014).
Aerosol particle and ion number-size distributions were measured by the station’s differential mobility particle sizer (DMPS, 3-1000 nm, 10 min time resolution; Aalto et al., 2001) and the NAIS (Manninen et al., 2009). Sub-3 nm particle number-size distribution was measured by a particle size magnifier running in scanning mode (PSM, 1.2-2.5 nm, 10 min time resolution; Vanhanen et al., 2011). Also a PSM measured at SPC but we were not able to reliably calculate formation rates from the data. Basic meteorological variables, radiation, and SO_2 were measured from the station’s mast at 16.8 meters above ground. In addition, a supporting NPF forecast tool was developed to aid the planning of research flights (Nieminen et al., 2015).

2.3 Zeppelin NT airship

A Zeppelin NT airship was used for monitoring the atmosphere below 1 km. The aerosol particles and trace gases were sampled with instrumentation installed inside the Zeppelin’s cabin. The Zeppelin operated with three different instrument layouts. A specific layout was chosen according to the flight plan and scientific aim of the flight.

Here we analyzed data from measurement flights that carried the so-called nucleation layout. Instruments specific to this layout were the atmospheric pressure interface time-of-flight mass spectrometer (APi-TOF; Junninen et al., 2010), used for measuring the elemental composition of naturally charged ions and the NAIS for particle and ion number size distributions. We also used the aerosol number-size distribution data from the SMPS (10-400 nm, 4 min time resolution) and PSM running in scanning mode, which were on board during all the measurement flights. The size range and time resolution of the onboard NAIS and PSM were same as for the instruments in HTL (see Section 2.1).

During a measurement flight the Zeppelin did multiple vertical profiles over a small area (~10 km^2). The profiling spot was picked typically down-wind from the measurement site in order not to compromise the ground-based measurements with any emissions. The vertical extent of the profiles was ~100-1000 m above the ground. The airspeed during measurement was ~20 m/s and the vertical speed during ascend and descend was ~0.5 m/s and ~3 m/s respectively.

2.4. Cessna 172 airplane

During the PEGASOS northern mission in spring 2013, a Cessna 172 airplane carrying scientific instrumentation was deployed to measure aerosol particles, trace gases and meteorological variables in the lower troposphere alongside the Zeppelin. The measurement setup and instrumentation on board have been described in previous studies (Lampilahti et al., 2020b; Schobesberger et al., 2013; Leino et al., 2019; Väänänen et al., 2016)

Basic meteorological variables (temperature, pressure, relative humidity) were measured on board. Particle number-size distribution was measured using a SMPS (10-400 nm size range, 2 min time resolution) and the number concentration of >3 nm particles was measured using an ultrafine condensation particle counter (UF-CPC, TSI model 3776) at 1 s time resolution. The altitude range of the airplane was ~100-3000 m above ground and the measurement airspeed was 36 m/s.

2.5 Flight profiles and atmospheric conditions

Our measurements focused on the time of BL development from sunrise until noon (Figure 1). This is the time when the onset of NPF is typically observed at the ground level. The vertical profile measurements represent the particle and gas concentrations in the lower parts of the atmosphere: the mixed layer, the residual layer, the nocturnal boundary layer. At the same time, the ground-based measurements recorded conditions in the surface layer. Here we consider the BL to include all the atmospheric layers below the free troposphere.

The basic conditions for the Zeppelin flights in both Italy and Finland were clear sky and low wind speed. Under these conditions, the sun heats the surface during the morning, which drives intense vertical mixing.

2.6 Data analysis

The onset of NPF occurs when low-volatility vapors in the atmosphere form nanometer sized clusters that continue to grow to larger aerosol particles (Kulmala et al., 2013).

We determined the onset of a NPF event visually from the initial increase in the number concentration of intermediate (2-4 nm) air ions at the beginning of the NPF event. An increase in the intermediate ion concentration has been identified as a good indicator for NPF (Leino et al., 2016). This is because an increase in the number concentration of intermediate ions is usually due to NPF and otherwise the number concentration is extremely low (below 5 cm^{-3}).

Particle growth rates (GR), formation rates and coagulation sinks were calculated in different size ranges according to the methods described by Kulmala et al. (2012). For particles and ions in the 1-2 nm and 2-3 nm size range the GR was determined from the ion number-size distribution measured by the NAIS. During NPF the number concentration in each size channel increased sequentially as the freshly formed particles grew larger. We determined the time when the number concentration began to rise in each size bin by fitting a sigmoid function to the rising concentration edge and finding the point where the sigmoid reached 75% of its maximum value (appearance time method; Lehtipalo et al., 2014). The corresponding diameter in each size bin was the bin's geometric mean diameter. Before the fitting procedure the number concentrations were averaged using a 15 min median and after that divided by the maximum concentration value in each size channel.

For larger particles and ions (3-7 nm and 7-20 nm) the GR was determined by fitting a log-normal distribution over the growing nucleation mode at each time step and assigning the fitted curve's peak value as the corresponding mode diameter. In each size range a value for the GR was obtained as the slope of a linear least squares fit to the time-diameter value pairs.

The formation rate of 1.5 nm particles and ions was determined from the PSM data and the NAIS ion data respectively (Kulmala et al., 2012). The formation rate of 3 nm particles and ions was determined from the NAIS data. Coagulation sinks were calculated from the SMPS or DMPS data. Condensation sink for sulfuric acid was calculated from the Zeppelin's on board SMPS.

Sulfuric acid (SA) is a key compound in atmospheric nucleation (Sipilä et al., 2010). As we did not have direct measurements of SA concentration, we used [HSO4-] from the APi-TOF measurements as a qualitative indicator of [H2SO4] and named it pseudo-SA. To determine this pseudo-SA, we summed up all ions containing HSO4-, e.g. the ion itself but also larger clusters, like $(H2SO4)_n$*HSO4-. We assumed steady state conditions and that the concentration of SA-containing ions is much lower than the total ion concentration. Under these conditions [HSO4-] (including all clusters where this ion was present) can be considered close to a linear function of [H2SO4] (Eisele and Tanner, 1991). At the highest SA loadings, ions with HSO4- can be a dominant fraction of the total ions (Ehn et al., 2010), in which case the linearity no longer holds. In addition, this assumes a constant concentration of ions, although for example the sinks for ions can vary, e.g. by an increased particle concentration. As such, the pseudo-SA parameter should indeed only be considered a qualitative indicator for SA.

In SPC the ML height was derived from the ceilometer measurements. However, in HTL weak scattering signal prevented reliable determination of ML height using the on-site lidar. For this reason in HTL the ML height was determined from vertical profiles of meteorological variables and aerosol particle concentrations on board the Zeppelin and the Cessna 172 airplane. In these profiles the top of the ML was revealed by the maximum positive gradient in potential temperature and minimum negative gradient in humidity and total particle number concentration (Stull, 1988).

The origin of the air masses was investigated using back trajectory analysis. The trajectories were calculated with the HYSPLIT (Hybrid Single Particle Lagrangian Integrated Trajectory; Stein et al., 2015) model using the GDAS (Global Data Assimilation System) archived data sets.

3 Results and discussion

3.1 Case study description

During the campaigns there were a limited number of flights with the nucleation instrument payload (Po Valley: 19.6.2012, 27.6.2012 , 28.6.2012 , 29. 6.2012 and 30.6.2012; Hyytiälä: 6.5.2013, 8.5.2013, 16.5.2013, 3.6.2013, 8.6.2013 and 10.6.2013). Here we present a side by side comparison of two case studies, one from SPC (June 28, 2012) and the other from HTL (May 8, 2013). On these days the NPF event was fully captured during the Zeppelin measurement. In addition the horizontal extent of NPF in SPC was investigated by studying the measurement flight from June 30, 2012.

June 28, 2012 was a hot and sunny day in Po Valley. 24-h back trajectories arriving to SPC during the morning revealed that the incoming air masses circulated from Central Europe and over the Adriatic Sea before arriving to SPC from the southwest (Figure 2a). Figure 3 shows the time series for some environmental parameters on the NPF event days from SPC and HTL. In SPC temperature and RH showed a large diurnal variation; the temperature increased from 16 °C to 32 °C during the morning while the RH decreased from 87% to 39%. The mean wind speed at 10 m height was 2.0 m s^{-1}. These meteorological conditions and air mass histories are common during NPF event days in Po Valley (Hamed et al., 2007; Sogacheva et al., 2007).

May 8, 2013 in HTL was a sunny and warm day with clear skies marked by broad diurnal variation in temperature and RH. During the morning the temperature increased from 5 °C to 17 °C and the RH decreased from 82% to 25%. The mean wind speed at 33.6 m height was 3.5 m s^{-1}. The air masses originated from the North Atlantic Ocean arriving to HTL from the northwest via Scandinavia and the Gulf of Bothnia (Figure 2b). Most NPF event days in HTL are clear sky days with the arriving air masses spending most of their time in the northwest sector (Dada et al., 2017; Nilsson et al., 2001; Sogacheva et al., 2008).

In SPC the solar radiation began to increase after 04:00 and according to the ceilometer measurements the ML started to increase in height around 06:00, at the same time the SO_2 concentration and $N_{>10}$ (number concentration of particles larger than 10 nm) began to increase. This is likely explained by the entrainment of pollutants from the RL and the onset of NPF. CS is higher during the night and decreases slightly during the day, which is likely due to dilution related to ML growth.

At HTL after sunrise the SO_2 concentration and $N_{>10}$ decreased probably due to the dilution caused by the growing ML coupled with the lack of pollution sources. While SO_2 concentration remained low the whole day, $N_{>10}$ and CS began to increase later during the day because of the NPF event. The average SO_2, $N_{>10}$ and CS in SPC were 0.57 ppb, 8102 cm^{-3} and 0.0128 s^{-1} respectively. While in HTL the corresponding values were 0.02 ppb, 3293 cm^{-3} and 0.0007 s^{-1}.

3.2 Onset of NPF

Figures 4a and 4b show the altitude of the Zeppelin as a function of time colored by the number concentration of intermediate ions measured by the NAIS at SPC and HTL. The plots also show the number concentration of intermediate ions measured on the ground as well as the ML height.

In SPC, the intermediate ion concentration began to increase on the ground at 5:48, which coincides with the beginning of convective mixing and the breakup of the nocturnal surface layer. Similarly, Kontkanen et al. (2016) observed that in Po Valley the onset of NPF coincided with the beginning of boundary layer growth. Around this time the Zeppelin was profiling the layers above the ML.

"Pockets" of elevated intermediate ion concentration were present inside the RL (for example around 700 m at 5:15). These pockets were not linked to the NPF event inside the ML. When the Zeppelin later entered the ML at around 6:45, NPF was already taking place throughout the developing ML and seemed to be confined to it.

In HTL, the number concentration of intermediate ions began to increase at around 6:47 on the ground level. The ML at this point had grown to around 600 m above ground, which allowed us to better resolve the onset of NPF vertically. In HTL no increase in intermediate ion concentration, indicating no NPF was observed above the ML on board the Zeppelin. Before 6:40 there was no sign of NPF inside the growing ML. Between 6:40 and 7:00 the Zeppelin briefly measured in the RL and re-entered the ML at 7:00. At this point the intermediate ion concentration was already increasing on board similar to the ground level, indicating the onset of NPF.

Figure 5 shows the intermediate ion number concentration as a function of time from the Zeppelin and the SMEAR II station. At the beginning of the NPF event, between 07:00-07:15, the Zeppelin ascended from 300 m to 800 m. During the ascend the intermediate ion concentrations increased at a similar rate and stayed at similar values on board the Zeppelin and at the ground level. The lack of vertical gradient in the number concentration suggests that the aerosol particles were forming homogeneously throughout the ML. However, intense turbulent mixing and strong updrafts moving up at roughly the same rate as the Zeppelin might have also resulted in a homogeneous number concentration, even if the aerosol particles were formed close to the surface.

Figures 4c and 4d show the Zeppelin's measurement profiles colored with the pseudo SA. In SPC, the highest amount of pseudo SA appears to be in the residual layer above the growing morning ML (also observed on June 27, 2012) after sunrise. This is in line with the observation that the SO_2 concentration increases at the surface when the ML starts to grow (Figure 3b), indicating that the SO_2 was entrained from the RL. The entrainment of SO_2 from the residual layer is also supported by previous observations (Kontkanen et al., 2016). The increased pseudo SA in the residual layer was not associated with NPF in the residual layer.
In SPC the night time SO_2 concentration at the surface is low likely due to deposition (Kontkanen et al., 2016). However ammonia concentration can be high (>30 μg m^{-3}) at the surface due to agricultural activities and the concentration has been observed to peak during the night and early morning (Sullivan et al., 2016). In addition oxidized VOCs are important for aerosol particle growth (Ehn et al., 2014). VOCs were measured on board the Zeppelin in Po Valley in 2012 and the results

showed higher VOC concentrations close to ground (Jäger, 2014). This may at least partly explain why we measured increased concentrations of intermediate ions in the RL but they did not appear to grow to larger sizes in any significant quantities.

Since in SPC the onset of NPF coincides with the beginning of ML growth, it is possible that the entrainment of SA from the residual layer into the growing ML where ammonia, and likely also amines from agricultural activities, are present can lead to stabilization of the SA clusters by the ammonia and amines and subsequent NPF (e.g. Almeida et al., 2013; Kirkby et al., 2011).

In SPC the pseudo-SA layer closely corresponded to a layer of reduced condensation sink (CS). In low CS regions more SA is in the gas phase and therefore detected by the APi-TOF (Figures 4e and 4f), which probably explains why the layer is there. In addition, the CS is also a sink for ions, which means that the pseudo-SA is likely decreased even more than SA, assuming that the loss rate is higher for ions than for SA molecules. By contrast, in HTL the amount of pseudo-SA is higher inside the ML than above it. The pseudo-SA concentration increases on board throughout the morning and peaks at roughly 9:00 and decreases afterwards.

In SPC pockets of intermediate ions and a layer of pseudo SA were observed in the RL, whereas at HTL intermediate ion concentrations and pseudo SA remained low in the RL. This is likely related to the relatively larger anthropogenic emissions in the Po Valley region compared to HTL. In previous studies NPF has been observed inside the RL in Central Europe (Wehner et al., 2010) and primary nanoparticles may be released into the RL from upwind pollution sources (Junkermann and Hacker, 2018).

3.2 Particle formation and growth rates

Figure 6 shows the number size distributions measured by the NAIS on board the Zeppelin and on the ground from SPC and HTL. The black dots are the mean mode diameters obtained by fitting a log-normal distribution over the growing particle mode.

In SPC, the number size distributions measured on board and on the ground with the NAIS (Figures 6a and 6c) were similar when the Zeppelin was measuring inside the ML. When the Zeppelin measured above the ML the number concentration decreased and the growing mode of freshly formed particles was not observed. The pockets of intermediate ions in the RL did not grow to larger sizes. This can be seen as sudden disappearances of the particles, for example at around 6:40, 7:15 and 8:00. The observations suggests that the NPF event was limited to the ML where it was taking place homogeneously.

We calculated the formation and growth rates in SPC and HTL for particles and ions on board the Zeppelin and on the ground. The results are summarized in Table 1. In SPC the onset of NPF happened when the ML was still very shallow and the Zeppelin was not measuring significant amount of time at this low altitude (this was a problem on other NPF event days from SPC as well), consequently the beginning of the NPF event was not fully observed on board. Because of this we were unable to reliably calculate the formation rates and the growth rate between 1-2 nm from the Zeppelin data.

Kontkanen et al. (2016) obtained formation rates of 23.5 $cm^{-3}\ s^{-1}$, 9.5 $cm^{-3}\ s^{-1}$, 0.1 $cm^{-3}\ s^{-1}$ and 0.08 $cm^{-3}\ s^{-1}$ for 1.5 nm particles, 2 nm particles, 2 nm positive ions and 2 nm negative ions respectively for the June 28, 2012 NPF event at the ground level. These values are in line with our values for the same day reported in Table 1 (J_3 = 6.8 cm^{-3}, J_3^- = 0.04 cm^{-3}, J_3^+ = 0.03 cm^{-3}). The higher formation rates in SPC compared to HTL are characteristic of polluted environments (Kerminen et al., 2018). The calculated GRs for the larger particle sizes as seen in Table 1 were similar on board the Zeppelin (HTL: $GR_{7\text{-}20}$ = 2.4 nm/h, SPC: $GR_{7\text{-}20}$ = 3.0 nm/h) and on the ground (HTL: $GR_{7\text{-}20}$ = 2.1 nm/h, SPC: $GR_{7\text{-}20}$ = 2.8 nm/h).

On May 8, 2013 in HTL almost the whole NPF event was captured by the Zeppelin measuring inside the ML. However, in contrast to SPC the number size distributions measured on board the Zeppelin (Figure 6b) and on the ground (Figure 6d) show differences, particularly in the growing nucleation mode particles. At different times on board the Zeppelin when it was measuring inside the ML the particle number concentration in the growing mode momentarily increased up to eight fold compared to the background number concentration, suggesting an enhancement in the particle formation rate. On board the Zeppelin this can be seen as concentrated "vertical stripes" in the number size distribution between 08:00-10:00. On the other hand at the ground station an increase of concentration of freshly formed particles was observed between 7:30-8:00. This inhomogeneity is further discussed in Section 3.3.

In the ground-based NAIS data a pool of sub-6 nm particles was present during the NPF event while on board the Zeppelin no such pool was observed. This can be seen most clearly between 10:00-11:30 when the median particle number concentration between 2-4 nm on the ground was

1400 cm^{-3} whereas on board the Zeppelin it was 570 cm^{-3}. Similarly Leino et al. (2019) observed that the number concentration of sub-3 nm particles decreases as a function of altitude at HTL. This may be linked to increased concentration of low-volatility vapors on the surface near the sources compared to aloft.

Despite the differences in the ground-based and airborne number size distributions in HTL a continuous, growing, nucleation mode was observed in the "background" both on the ground (alongside the pool of sub-6 nm particles) and on board the Zeppelin during the NPF event. When averaged over the total duration of the NPF event, the growth rates and formation rates on board the Zeppelin and on the ground were similar on this day. This would indicate that the ground-based measurements represent the NPF event in the whole ML quite well. However locally increased number concentrations, indicating enhanced NPF, were observed inside the ML and if the enhancement is not detected with the ground-based measurements we may underestimate the intensity of NPF within the ML based on ground-based data alone.

3.3 Vertical and horizontal distribution of the freshly formed particles

Next we investigated how the freshly formed particles were distributed spatially in the BL. Figure 6e shows the particle number concentration between 3-10 nm measured by the NAIS and the ML height from SPC as a function of time and altitude. The freshly formed particles were distributed homogeneously throughout the growing ML but were not found in the RL. The 3-10 nm number concentration inside the ML was ~20 000 cm^{-3} while in the residual layer it was only ~200 cm^{-3}. The pockets of increased intermediate ion concentration, indicating NPF in the nocturnal boundary layer and residual layer (Figure 4a), were not observed in the 3-10 nm size range suggesting that the particles did not grow to the 3-10 nm size range in any significant numbers.

At HTL the Zeppelin was measuring in the lower half of the developed ML, however the Cessna profiled the entire depth of the ML all the way up to the lower parts of the free troposphere. Figure 7 shows the vertical profile of 3-10 nm particle number concentration between 07:00-10:00 UTC calculated by subtracting the total SMPS number concentration from the UF-CPC number concentration on board the Cessna. Also the water vapor concentration and temperature are shown. A temperature inversion, a large negative gradient in water vapor concentration and in the particle number concentration indicated that the top of the ML was present between 1300-1400 m.

On average the number concentration inside the ML remained roughly constant ($N_{3\text{-}10}$ ~1000 cm^{-3}) as a function of altitude, however there was substantial variation (~200-3000 cm^{-3}). The strongest variation came from a narrow sector roughly at the center of the measurement area, which is discussed below. The NPF did not extend to the RL where the number concentrations were reduced to below 100 cm^{-3}.

However at 2000 m a layer of sub-10 nm particles was observed. The 3-10 nm number concentration increased from less than 100 cm^{-3} to ~400 cm^{-3}. Lampilahti et al. (2021) showed evidence that NPF frequently takes place in the interface between the residual layer and the free troposphere, disconnected from the ML. Precursor gases may be transported to these altitudes and the mixing over the interface layer could initiate nucleation.

Figure 8a shows the particle number concentration between 3-10 nm on board the Zeppelin and the airplane as a function of longitude and latitude from HTL on May 8, 2013. The particle number concentration was elevated right over HTL in a narrow sector perpendicular to the mean wind direction. Vertically the sector extended throughout the depth of the ML. The number concentration in the sector increased 2-8 fold compared to the surrounding background number concentration. The mean wind speed in the ML was about 4 m/s and the particle sector was observed throughout the whole measurement flight, for at least 2.5 hours. This suggests that the particle sector was probably at least 35 km long along the mean wind direction.

The concentrated vertical stripes over the growing nucleation mode in Figure 6b were caused by the Zeppelin periodically flying through the particle sector. The sector slowly moved perpendicular to the mean wind towards northeast and when passing over HTL it was seen as the plume of particles in Figure 6d between 07:30-08:00. The particles in the sector grew at approximately the same rate with the background NPF event particles, which also suggests that the particles were formed simultaneously inside the long and narrow sector. Lampilahti et al. (2020b) showed that these types of NPF events, or local enhancements of regional NPF events, are common in HTL and that they are linked to roll vortices, which are a specific mode of organized convection in the BL.

On June 28, 2012 in SPC the Zeppelin flew the measurement profiles over a small area and therefore it was difficult to infer the horizontal extent of the NPF event. However, on June 30, 2012 the Zeppelin measured over a larger area in order to find the edges of the airmass where the NPF event was taking place. The flight on June 30, 2012 lasted from 05:00 to 10:00 UTC. Figure 9b shows that the NPF event was observed to occur in the sector of the Valley comprised between Ozzano (just north of the Apennine foothills) and the city of Ferrara (just south of the Po river). The area in between experienced westerly winds, from the inner Po Valley toward the Adriatic sea, which is a common feature of the Po Valley wind breeze system in the early morning.

Farther north of the Po river, an easterly breeze was developing and no NPF was observed (off the map in Figure 8b, see Figure 9). Nocturnal north-easterly breezes are often observed over the Three Venezie Plain as a result of a low-level jet (Camuffo et al., 1979). The variability in local wind fields may generate chemical gradients in the atmospheric surface layer within the Po Valley, hence segregating air masses which can be active or inactive with respect to NPF, in complete absence of orographic forcings (i.e. over a completely flat terrain). Probably the air masses with an easterly component reaching the Zeppelin from the Venetian plain picked up pollution (e.g. CO, NO_x) from urban sources, but we can also speculate that for example ammonia and amines were much lower than in the westerly air masses flowing south of the Po river, which had crossed the areas between Emilia and Lombardy where most agricultural activities take place (see Figure 9). A chemical transport model run predicting NH_3 concentrations with adequate resolution, and using them as a tracer for the actual precursors for NPF, might clarify this point. However modeling atmospheric transport at this scale in an environment like Po Valley can have substantial uncertainties (Vogel and Elbern, 2021).

4 Conclusions

Flight measurements are essential to evaluate the representativeness of the ground-based in-situ measurements. In many cases it may be impossible to tell from only ground-based data what drives the observed NPF, especially when the effect of BL dynamics is important. Atmospheric models require field observations for validation and constraints. Airborne measurements such as the ones reported here provide valuable data for this purpose.

We compared case studies from two different environments where NPF occurs frequently: a suburban area in Po Valley, Italy, and a boreal forest in Hyytiälä, Finland. We aimed to answer in which part of the BL the onset of NPF and the growth of the freshly formed particles took place and studied the vertical and horizontal extent of NPF.

To detect directly the very first steps of NPF in the BL, we used airborne Zeppelin and airplane measurements, supported by ground-based in-situ measurements. The Zeppelin measurements allowed us to study the vertical extent of NPF in the BL. The high time resolution and low cut-off size of the instruments on board allowed us to observe the starting time, location and altitude of an NPF event.

Within the limits of the Zeppelin's vertical profiling speed (~ 0.5 m/s ascend) and the time resolution of the NAIS, we observed that the onset of NPF happened simultaneously inside the ML. However particles formed close to the surface could probably still be mixed by strong updrafts fast enough so that the number concentrations measured on board the Zeppelin appear homogeneous. The newly formed particles were observed to grow to larger sizes at the same rate within the ML. However, in HTL we observed local enhancements in NPF that were induced by roll vortices in the BL.

In addition a separate layer of sub-10 nm particles was observed above the ML in HTL. Lampilahti et al. (2021) showed that such layers in HTL are likely the result of NPF in the topmost part of the RL. Furthermore it was estimated that around 42% of the NPF events observed in HTL at the surface are entrained from such elevated layers. In SPC we observed how NPF could be happening in one air mass but be completely absent in an adjacent air mass with a different origin.

The conditions on our case study days represent the typical conditions in these locations when NPF events usually occur. That is to say, a sunny day with the air masses originating from a certain area during a specific time of the year (May in HTL and June in SPC) when NPF is common. Nevertheless it is not certain that our case studies represent a typical NPF event day. NPF events also occur under different kinds of conditions. The growing nucleation mode particles originating from NPF do not always grow smoothly and continuously in the measured size distribution like in our cases, but may have large variation and discontinuities, which may reflect the vertical and horizontal variability in NPF.

Acknowledgements

This research was supported by the European Commission under the Framework Programme 7 (FP7-ENV-2010-265148). The support by the Academy of Finland Centre of Excellence program (project no. 272041 and 1118615), the ERC-Advanced "ATMNUCLE" (grant no. 227463), the Eurostars Programme (contract no. E!6911), and the Finnish Cultural Foundation is also gratefully acknowledged. The Zeppelin is accompanied by an international team of scientists and technicians. They are all warmly acknowledged.

Data availability. Data used in this study is available from different sources: Ground-based meteorological data, radiation, gas and particle size distribution data from HTL (Junninen et al., 2009), the Cessna dataset (Lampilahti et al., 2020a) and the rest of the data (Lampilahti et al., 2021b).

Author contributions. HM, TN, SM, ME, IP, SS, JKa, EJ, TYJ, RK, KLeh, SD, AM, RT, DW, FR, TP, TM and MK coordinated the Zeppelin campaign. RV carried out the Cessna measurements. JLa, TN, HM, JKo, KLei and VMK analyzed and interpreted the data. JL and HM prepared the manuscript, with contributions from all coauthors.

The authors declare that they have no conflict of interest.

References

Aalto, P., Hämeri, K., Becker, E., Weber, R., Salm, J., Mäkelä, J. M., Hoell, C., O'Dowd, C. D., Hansson, H.-C., Väkevä, M., Koponen, I. K., Buzorius, G., and Kulmala, M.: Physical characterization of aerosol particles during nucleation events, Tellus B, 53, 344–358, https://doi.org/10.3402/tellusb.v53i4.17127, 2001.

Almeida, J., Schobesberger, S., Kürten, A., Ortega, I. K., Kupiainen-Määttä, O., Praplan, A. P., Adamov, A., Amorim, A., Bianchi, F., Breitenlechner, M., David, A., Dommen, J., Donahue, N. M., Downard, A., Dunne, E., Duplissy, J., Ehrhart, S., Flagan, R. C., Franchin, A., Guida, R., Hakala, J., Hansel, A., Heinritzi, M., Henschel, H., Jokinen, T., Junninen, H., Kajos, M., Kangasluoma, J., Keskinen, H., Kupc, A., Kurtén, T., Kvashin, A. N., Laaksonen, A., Lehtipalo, K., Leiminger, M., Leppä, J., Loukonen, V., Makhmutov, V., Mathot, S., McGrath, M. J., Nieminen, T., Olenius, T., Onnela, A., Petäjä, T., Riccobono, F., Riipinen, I., Rissanen, M., Rondo, L., Ruuskanen, T., Santos, F. D., Sarnela, N., Schallhart, S., Schnitzhofer, R., Seinfeld, J. H., Simon, M., Sipilä, M., Stozhkov, Y., Stratmann, F., Tomé, A., Tröstl, J., Tsagkogeorgas, G., Vaattovaara, P., Viisanen, Y., Virtanen, A., Vrtala, A., Wagner, P. E., Weingartner, E., Wex, H., Williamson, C., Wimmer, D., Ye, P., Yli-Juuti, T., Carslaw, K. S., Kulmala, M., Curtius, J., Baltensperger, U., Worsnop, D. R., Vehkamäki, H., and Kirkby, J.: Molecular understanding of sulphuric acid-amine particle nucleation in the atmosphere, Nature, 502, 359–363, https://doi.org/10.1038/nature12663, 2013.

Camuffo, D., Tampieri, F., and Zambon, G.: Local mesoscale circulation over Venice as a result of the mountain-sea interaction, Bound.-Layer Meteorol., 16, 83–92, https://doi.org/10.1007/BF02220408, 1979.

Chen, H., Hodshire, A. L., Ortega, J., Greenberg, J., McMurry, P. H., Carlton, A. G., Pierce, J. R., Hanson, D. R., and Smith, J. N.: Vertically resolved concentration and liquid water content of atmospheric nanoparticles at the US DOE Southern Great Plains site, Atmospheric Chem. Phys., 18, 311–326, https://doi.org/10.5194/acp-18-311-2018, 2018.

Dada, L., Paasonen, P., Nieminen, T., Buenrostro Mazon, S., Kontkanen, J., Peräkylä, O., Lehtipalo, K., Hussein, T., Petäjä, T., Kerminen, V.-M., Bäck, J., and Kulmala, M.: Long-term analysis of clear-sky new particle formation events and nonevents in Hyytiälä, Atmos Chem Phys, 17, 6227–6241, https://doi.org/10.5194/acp-17-6227-2017, 2017.

Dal Maso, M., Kulmala, M., Riipinen, I., Wagner, R., Hussein, T., Aalto, P. P., and Lehtinen, K. E.: Formation and growth of fresh atmospheric aerosols: eight years of aerosol size distribution data from SMEAR II, Hyytiälä, Finland, Boreal Environ. Res., 10, 323, 2005.

Dunne, E. M., Gordon, H., Kürten, A., Almeida, J., Duplissy, J., Williamson, C., Ortega, I. K., Pringle, K. J., Adamov, A., Baltensperger, U., Barmet, P., Benduhn, F., Bianchi, F., Breitenlechner, M., Clarke, A., Curtius, J., Dommen, J., Donahue, N. M., Ehrhart, S., Flagan, R. C., Franchin, A., Guida, R., Hakala, J., Hansel, A., Heinritzi, M., Jokinen, T., Kangasluoma, J., Kirkby, J., Kulmala, M., Kupc, A., Lawler, M. J., Lehtipalo, K., Makhmutov, V., Mann, G., Mathot, S., Merikanto, J., Miettinen, P., Nenes, A., Onnela, A., Rap, A., Reddington, C. L. S., Riccobono, F., Richards, N. A. D., Rissanen, M. P., Rondo, L., Sarnela, N., Schobesberger, S., Sengupta, K., Simon, M., Sipilä, M., Smith, J. N., Stozkhov, Y., Tomé, A., Tröstl, J., Wagner, P. E., Wimmer, D., Winkler, P. M., Worsnop, D. R., and Carslaw, K. S.: Global atmospheric particle formation from CERN CLOUD measurements, Science, 354, 1119–1124, https://doi.org/10.1126/science.aaf2649, 2016.

Ehn, M., Junninen, H., Petäjä, T., Kurtén, T., Kerminen, V.-M., Schobesberger, S., Manninen, H. E., Ortega, I. K., Vehkamäki, H., Kulmala, M., and Worsnop, D. R.: Composition and temporal behavior of ambient ions in the boreal forest, Atmospheric Chem. Phys., 10, 8513–8530, https://doi.org/10.5194/acp-10-8513-2010, 2010.

Ehn, M., Thornton, J. A., Kleist, E., Sipilä, M., Junninen, H., Pullinen, I., Springer, M., Rubach, F., Tillmann, R., Lee, B., Lopez-Hilfiker, F., Andres, S., Acir, I.-H., Rissanen, M., Jokinen, T., Schobesberger, S., Kangasluoma, J., Kontkanen, J., Nieminen, T., Kurtén, T., Nielsen, L. B., Jørgensen, S., Kjaergaard, H. G., Canagaratna, M., Maso, M. D., Berndt, T., Petäjä, T., Wahner, A., Kerminen, V.-M., Kulmala, M., Worsnop, D. R., Wildt, J., and Mentel, T. F.: A large source of low-volatility secondary organic aerosol, Nature, 506, 476–479, https://doi.org/10.1038/nature13032, 2014.

Eisele, F. L. and Tanner, D. J.: Ion-assisted tropospheric OH measurements, J. Geophys. Res. Atmospheres, 96, 9295–9308, https://doi.org/10.1029/91JD00198, 1991.

Gordon, H., Kirkby, J., Baltensperger, U., Bianchi, F., Breitenlechner, M., Curtius, J., Dias, A., Dommen, J., Donahue, N. M., Dunne, E. M., Duplissy, J., Ehrhart, S., Flagan, R. C., Frege, C., Fuchs, C., Hansel, A., Hoyle, C. R., Kulmala, M., Kürten, A., Lehtipalo, K., Makhmutov, V., Molteni, U., Rissanen, M. P., Stozkhov, Y., Tröstl, J., Tsagkogeorgas, G., Wagner, R., Williamson, C., Wimmer, D., Winkler, P. M., Yan, C., and Carslaw, K. S.: Causes and importance of new particle formation in the present-day and preindustrial atmospheres, J. Geophys. Res. Atmospheres, 122, 8739–8760, https://doi.org/10.1002/2017JD026844, 2017.

Hakola, H., Tarvainen, V., Laurila, T., Hiltunen, V., Hellén, H., and Keronen, P.: Seasonal variation of VOC concentrations above a boreal coniferous forest, Atmos. Environ., 37, 1623–1634, https://doi.org/10.1016/S1352-2310(03)00014-1, 2003.

Hamed, A., Joutsensaari, J., Mikkonen, S., Sogacheva, L., Maso, M. D., Kulmala, M., Cavalli, F., Fuzzi, S., Facchini, M. C., Decesari, S., Mircea, M., Lehtinen, K. E. J., and Laaksonen, A.: Nucleation and growth of new particles in Po Valley, Italy, Atmospheric Chem. Phys., 7, 355–376, https://doi.org/10.5194/acp-7-355-2007, 2007.

Hari, P. and Kulmala, M.: Station for measuring ecosystem-atmosphere relations (SMEAR II), Boreal Environ. Res., 10, 315–322, 2005.

Jäger, J.: Airborne VOC measurements on board the Zeppelin NT during the PEGASOS campaigns in 2012 deploying the improved Fast-GC-MSD System, Forschungszentrum Jülich GmbH, 2014.

Junkermann, W. and Hacker, J. M.: Ultrafine Particles in the Lower Troposphere: Major Sources, Invisible Plumes, and Meteorological Transport Processes, Bull. Am. Meteorol. Soc., 99, 2587–2602, https://doi.org/10.1175/BAMS-D-18-0075.1, 2018.

Junninen, H., Lauri, A., Keronen, P., AaIto, P., HiItunen, V., Hari, P., and KuImaIa, M.: Smart-SMEAR: on-line data exploration and visualization tool tor SMEAR stations., Boreal Environ. Res., 14, 447–457, 2009.

Junninen, H., Ehn, M., Petäjä, T., Luosujärvi, L., Kotiaho, T., Kostiainen, R., Rohner, U., Gonin, M., Fuhrer, K., Kulmala, M., and Worsnop, D. R.: A high-resolution mass spectrometer to measure atmospheric ion composition, Atmospheric Meas. Tech., 3, 1039–1053, https://doi.org/10.5194/amt-3-1039-2010, 2010.

Kerminen, V.-M., Chen, X., Vakkari, V., Petäjä, T., Kulmala, M., and Bianchi, F.: Atmospheric new particle formation and growth: review of field observations, Environ. Res. Lett., 13, 103003, https://doi.org/10.1088/1748-9326/aadf3c, 2018.

Kirkby, J., Curtius, J., Almeida, J., Dunne, E., Duplissy, J., Ehrhart, S., Franchin, A., Gagné, S., Ickes, L., Kürten, A., Kupc, A., Metzger, A., Riccobono, F., Rondo, L., Schobesberger, S., Tsagkogeorgas, G., Wimmer, D., Amorim, A., Bianchi, F., Breitenlechner, M., David, A., Dommen, J., Downard, A., Ehn, M., Flagan, R. C., Haider, S., Hansel, A., Hauser, D., Jud, W., Junninen, H., Kreissl, F., Kvashin, A., Laaksonen, A., Lehtipalo, K., Lima, J., Lovejoy, E. R., Makhmutov, V., Mathot, S., Mikkilä, J., Minginette, P., Mogo, S., Nieminen, T., Onnela, A., Pereira, P., Petäjä, T., Schnitzhofer, R., Seinfeld, J. H., Sipilä, M., Stozhkov, Y., Stratmann, F., Tomé, A., Vanhanen, J., Viisanen, Y., Vrtala, A., Wagner, P. E., Walther, H., Weingartner, E., Wex, H., Winkler, P. M., Carslaw, K. S., Worsnop, D. R., Baltensperger, U., and Kulmala, M.: Role of sulphuric acid, ammonia and galactic cosmic rays in atmospheric aerosol nucleation, Nature, 476, 429–433, https://doi.org/10.1038/nature10343, 2011.

Kontkanen, J., Järvinen, E., Manninen, H. E., Lehtipalo, K., Kangasluoma, J., Decesari, S., Gobbi, G. P., Laaksonen, A., Petäjä, T., and Kulmala, M.: High concentrations of sub-3nm clusters and frequent new particle formation observed in the Po Valley, Italy, during the PEGASOS 2012 campaign, http://dx.doi.org/10.5194/acp-16-1919-2016, 2016.

Kulmala, M., Petäjä, T., Nieminen, T., Sipilä, M., Manninen, H. E., Lehtipalo, K., Dal Maso, M., Aalto, P. P., Junninen, H., Paasonen, P., Riipinen, I., Lehtinen, K. E. J., Laaksonen, A., and Kerminen, V.-M.: Measurement of the nucleation of atmospheric aerosol particles, Nat. Protoc., 7, 1651–1667, https://doi.org/10.1038/nprot.2012.091, 2012.

Kulmala, M., Kontkanen, J., Junninen, H., Lehtipalo, K., Manninen, H. E., Nieminen, T., Petäjä, T., Sipilä, M., Schobesberger, S., Rantala, P., Franchin, A., Jokinen, T., Järvinen, E., Äijälä, M., Kangasluoma, J., Hakala, J., Aalto, P. P., Paasonen, P., Mikkilä, J., Vanhanen, J., Aalto, J., Hakola, H., Makkonen, U., Ruuskanen, T., Mauldin, R. L., Duplissy, J., Vehkamäki, H., Back, J., Kortelainen, A., Riipinen, I., Kurten, T., Johnston, M. V., Smith, J. N., Ehn, M., Mentel, T. F., Lehtinen, K. E. J., Laaksonen, A., Kerminen, V.-M., and Worsnop, D. R.: Direct observations of atmospheric aerosol nucleation, Science, 339, 943–946, https://doi.org/10.1126/science.1227385, 2013.

Laakso, L., Grönholm, T., Kulmala, L., Haapanala, S., Hirsikko, A., Lovejoy, E. R., Kazil, J., Kurten, T., Boy, M., Nilsson, E. D., Sogachev, A., Riipinen, I., Stratmann, F., and Kulmala, M.: Hot-air balloon as a platform for boundary layer profile measurements during particle formation, Boreal Environ. Res., 12, 279–294, 2007.

Laaksonen, A., Hamed, A., Joutsensaari, J., Hiltunen, L., Cavalli, F., Junkermann, W., Asmi, A., Fuzzi, S., and Facchini, M. C.: Cloud condensation nucleus production from nucleation events at a highly polluted region, Geophys. Res. Lett., 32, https://doi.org/10.1029/2004GL022092, 2005.

Lampilahti, J., Manninen, H. E., Leino, K., Väänänen, R., Manninen, A., Buenrostro Mazon, S., Nieminen, T., Leskinen, M., Enroth, J., Bister, M., Zilitinkevich, S., Kangasluoma, J., Järvinen, H., Kerminen, V.-M., Petäjä, T., and Kulmala, M.: Data set of airborne and ground-based atmospheric measurements from Hyytiälä, Finland, https://doi.org/10.5281/zenodo.3688471, 2020a.

Lampilahti, J., Manninen, H. E., Leino, K., Väänänen, R., Manninen, A., Buenrostro Mazon, S., Nieminen, T., Leskinen, M., Enroth, J., Bister, M., Zilitinkevich, S., Kangasluoma, J., Järvinen, H., Kerminen, V.-M., Petäjä, T., and Kulmala, M.: Roll vortices induce new particle formation bursts in the planetary boundary layer, Atmospheric Chem. Phys., 20, 11841–11854, https://doi.org/10.5194/acp-20-11841-2020, 2020b.

Lampilahti, J., Leino, K., Manninen, A., Poutanen, P., Franck, A., Peltola, M., Hietala, P., Beck, L., Dada, L., Quéléver, L., Öhrnberg, R., Zhou, Y., Ekblom, M., Vakkari, V., Zilitinkevich, S., Kerminen, V.-M., Petäjä, T., and Kulmala, M.: Aerosol particle formation in the upper residual layer, Atmospheric Chem. Phys., 21, 7901–7915, https://doi.org/10.5194/acp-21-7901-2021, 2021a.

Lampilahti, J., Manninen, H. E., Nieminen, T., Mirme, S., Ehn, M., Pullinen, I., Leino, K., Schobesberger, S., Kangasluoma, J., Kontkanen, J., Järvinen, E., Väänänen, R., Yli-Juuti, T., Krecji, R., Lehtipalo, K., Levula, J., Mirme, A., Decesari, S., Tillmann, R., Worsnop, D. R., Rohrer, F., Petäjä, T., Kerminen, V.-M., Mentel, T. F., and Kulmala, M.: Zeppelin-led study on the onset of new particle formation in the planetary boundary layer: dataset, https://doi.org/10.5281/zenodo.4660145, 2021b.

Lehtipalo, K., Leppä, J., Kontkanen, J., Kangasluoma, J., Franchin, A., Wimmer, D., Schobesberger, S., Junninen, H., Petäjä, T., Sipilä, M., Mikkilä, J., Vanhanen, J., Worsnop, D. R., and Kulmala, M.: Methods for determining particle size distribution and growth rates between 1 and 3 nm using the Particle Size Magnifier, Boreal Environ. Res., 19, 22, 2014.

Leino, K., Nieminen, T., Manninen, H. E., Petäjä, T., Kerminen, V.-M., and Kulmala, M.: Intermediate ions as a strong indicator for new particle formation bursts in boreal forest, Boreal Environ. Res., 21, 274–286, 2016.

Leino, K., Lampilahti, J., Poutanen, P., Väänänen, R., Manninen, A., Buenrostro Mazon, S., Dada, L., Franck, A., Wimmer, D., Aalto, P. P., Ahonen, L. R., Enroth, J., Kangasluoma, J., Keronen, P., Korhonen, F., Laakso, H., Matilainen, T., Siivola, E., Manninen, H. E., Lehtipalo, K., Kerminen, V.-M., Petäjä, T., and Kulmala, M.: Vertical profiles of sub-3 nm particles over the boreal forest, Atmospheric Chem. Phys., 19, 4127–4138, https://doi.org/10.5194/acp-19-4127-2019, 2019.

Manninen, H. E., Petäjä, T., Asmi, E., Riipinen, N., Nieminen, T., Mikkilä, J., Horrak, U., Mirme, A., Mirme, S., Laakso, L., Kerminen, V.-M., and Kulmala, M.: Long-term field measurements of charged and neutral clusters using Neutral cluster and Air Ion Spectrometer (NAIS), Boreal Environ. Res., 14, 591–605, 2009.

Mirme, S. and Mirme, A.: The mathematical principles and design of the NAIS – a spectrometer for the measurement of cluster ion and nanometer aerosol size distributions, Atmospheric Meas. Tech., 6, 1061–1071, https://doi.org/10.5194/amt-6-1061-2013, 2013.

Mohr, C., Thornton, J. A., Heitto, A., Lopez-Hilfiker, F. D., Lutz, A., Riipinen, I., Hong, J., Donahue, N. M., Hallquist, M., Petäjä, T., Kulmala, M., and Yli-Juuti, T.: Molecular identification of organic vapors driving atmospheric nanoparticle growth, Nat. Commun., 10, 4442, https://doi.org/10.1038/s41467-019-12473-2, 2019.

Nieminen, T., Asmi, A., Dal Maso, M., Aalto, P. P., Keronen, P., Petäjä, T., Kulmala, M., and Kerminen, V.-M.: Trends in atmospheric new-particle formation: 16 years of observations in a boreal-forest environment, Boreal Environ. Res., 19, 191–214, 2014.

Nieminen, T., Yli-Juuti, T., Manninen, H. E., Petäjä, T., Kerminen, V.-M., and Kulmala, M.: Technical note: New particle formation event forecasts during PEGASOS–Zeppelin Northern mission 2013 in Hyytiälä, Finland, Atmospheric Chem. Phys., 15, 12385–12396, https://doi.org/10.5194/acp-15-12385-2015, 2015.

Nilsson, E. D., Rannik, Ü., Kulmala, M., Buzorius, G., and O'dowd, C. D.: Effects of continental boundary layer evolution, convection, turbulence and entrainment, on aerosol formation, Tellus B, 53, 441–461, https://doi.org/10.1034/j.1600-0889.2001.530409.x, 2001.

O'Dowd, C. D., Yoon, Y. J., Junkermann, W., Aalto, P., Kulmala, M., Lihavainen, H., and Viisanen, Y.: Airborne measurements of nucleation mode particles II: boreal forest nucleation events, Atmospheric Chem. Phys., 9, 937–944, https://doi.org/10.5194/acp-9-937-2009, 2009.

Pierce, J. R. and Adams, P. J.: Uncertainty in global CCN concentrations from uncertain aerosol nucleation and primary emission rates, Atmospheric Chem. Phys., 9, 1339–1356, https://doi.org/10.5194/acp-9-1339-2009, 2009.

Platis, A., Altstädter, B., Wehner, B., Wildmann, N., Lampert, A., Hermann, M., Birmili, W., and Bange, J.: An Observational Case Study on the Influence of Atmospheric Boundary-Layer Dynamics on New Particle Formation, Bound.-Layer Meteorol., 158, 67–92, https://doi.org/10.1007/s10546-015-0084-y, 2015.

Schobesberger, S., Väänänen, R., Leino, K., Virkkula, A., Backman, J., Pohja, T., Siivola, E., Franchin, A., Mikkilä, J., Paramonov, M., Aalto, P. P., Krejci, R., Petäjä, T., and Kulmala, M.: Airborne measurements over the boreal forest of southern Finland during new particle formation events in 2009 and 2010, Boreal Environ. Res., 18, 145–164, 2013.

Siebert, H., Stratmann, F., and Wehner, B.: First observations of increased ultrafine particle number concentrations near the inversion of a continental planetary boundary layer and its relation to ground-based measurements, Geophys. Res. Lett., 31, L09102, https://doi.org/10.1029/2003GL019086, 2004.

Sipilä, M., Berndt, T., Petäjä, T., Brus, D., Vanhanen, J., Stratmann, F., Patokoski, J., Mauldin, R. L., Hyvärinen, A.-P., Lihavainen, H., and Kulmala, M.: The Role of Sulfuric Acid in Atmospheric Nucleation, Science, 327, 1243–1246, https://doi.org/10.1126/science.1180315, 2010.

Sogacheva, L., Hamed, A., Facchini, M. C., Kulmala, M., and Laaksonen, A.: Relation of air mass history to nucleation events in Po Valley, Italy, using back trajectories analysis, Atmos Chem Phys, 7, 839–853, https://doi.org/10.5194/acp-7-839-2007, 2007.

Sogacheva, L., Saukkonen, L., Nilsson, E. D., Dal Maso, M., Schultz, D. M., De Leeuw, G., and Kulmala, M.: New aerosol particle formation in different synoptic situations at Hyytiälä, Southern Finland, Tellus B, 60, 485–494, https://doi.org/10.1111/j.1600-0889.2008.00364.x, 2008.

Stein, A. F., Draxler, R. R., Rolph, G. D., Stunder, B. J. B., Cohen, M. D., and Ngan, F.: NOAA's HYSPLIT Atmospheric Transport and Dispersion Modeling System, Bull. Am. Meteorol. Soc., 96, 2059–2077, https://doi.org/10.1175/BAMS-D-14-00110.1, 2015.

Stratmann, F., Siebert, H., Spindler, G., Wehner, B., Althausen, D., Heintzenberg, J., Hellmuth, O., Rinke, R., Schmieder, U., Seidel, C., Tuch, T., Uhrner, U., Wiedensohler, A., Wandinger, U., Wendisch, M., Schell, D., and Stohl, A.: New-particle formation events in a continental boundary layer: first results from the SATURN experiment, Atmospheric Chem. Phys., 3, 1445–1459, https://doi.org/10.5194/acp-3-1445-2003, 2003.

Stull, R. B.: An Introduction to Boundary Layer Meteorology, Softcover reprint of the original 1st ed. 1988 edition., Springer, Dordrecht, 670 pp., 1988.

Sullivan, A. P., Hodas, N., Turpin, B. J., Skog, K., Keutsch, F. N., Gilardoni, S., Paglione, M., Rinaldi, M., Decesari, S., Facchini, M. C., Poulain, L., Herrmann, H., Wiedensohler, A., Nemitz, E., Twigg, M. M., and Collett Jr., J. L.: Evidence for ambient dark aqueous SOA formation in the Po Valley, Italy, Atmospheric Chem. Phys., 16, 8095–8108, https://doi.org/10.5194/acp-16-8095-2016, 2016.

Väänänen, R., Krejci, R., Manninen, H. E., Manninen, A., Lampilahti, J., Buenrostro Mazon, S., Nieminen, T., Yli-Juuti, T., Kontkanen, J., Asmi, A., Aalto, P. P., Keronen, P., Pohja, T., O'Connor, E., Kerminen, V.-M., Petäjä, T., and Kulmala, M.: Vertical and horizontal variation of aerosol number size distribution in the boreal environment, Atmospheric Chem. Phys. Discuss., Manuscript in review, https://doi.org/10.5194/acp-2016-556, 2016.

Vanhanen, J., Mikkilä, J., Lehtipalo, K., Sipilä, M., Manninen, H. E., Siivola, E., Petäjä, T., and Kulmala, M.: Particle size magnifier for nano-CN detection, Aerosol Sci. Technol., 45, 533–542, https://doi.org/10.1080/02786826.2010.547889, 2011.

Vogel, A. and Elbern, H.: Identifying forecast uncertainties for biogenic gases in the Po Valley related to model configuration in EURAD-IM during PEGASOS 2012, Atmospheric Chem. Phys., 21, 4039–4057, https://doi.org/10.5194/acp-21-4039-2021, 2021.

Wehner, B., Siebert, H., Ansmann, A., Ditas, F., Seifert, P., Stratmann, F., Wiedensohler, A., Apituley, A., Shaw, R. A., Manninen, H. E., and Kulmala, M.: Observations of turbulence-induced new particle formation in the residual layer, Atmospheric Chem. Phys., 10, 4319–4330, https://doi.org/10.5194/acp-10-4319-2010, 2010.

Wiedensohler, A., Birmili, W., Nowak, A., Sonntag, A., Weinhold, K., Merkel, M., Wehner, B., Tuch, T., Pfeifer, S., Fiebig, M., Fjäraa, A. M., Asmi, E., Sellegri, K., Depuy, R., Venzac, H., Villani, P., Laj, P., Aalto, P., Ogren, J. A., Swietlicki, E., Williams, P., Roldin, P., Quincey, P., Hüglin, C., Fierz-Schmidhauser, R., Gysel, M., Weingartner, E., Riccobono, F., Santos, S., Grüning, C., Faloon, K., Beddows, D., Harrison, R., Monahan, C., Jennings, S. G., O'Dowd, C. D., Marinoni, A., Horn, H.-G., Keck, L., Jiang, J., Scheckman, J., McMurry, P. H., Deng, Z., Zhao, C. S., Moerman, M., Henzing, B., de Leeuw, G., Löschau, G., and Bastian, S.: Mobility particle size spectrometers: harmonization of technical standards and data structure to facilitate high quality long-term observations of atmospheric particle number size distributions, Atmospheric Meas. Tech., 5, 657–685, https://doi.org/10.5194/amt-5-657-2012, 2012.

Yu, F. and Luo, G.: Simulation of particle size distribution with a global aerosol model: contribution of nucleation to aerosol and CCN number concentrations, Atmospheric Chem. Phys., 9, 7691–7710, 2009.

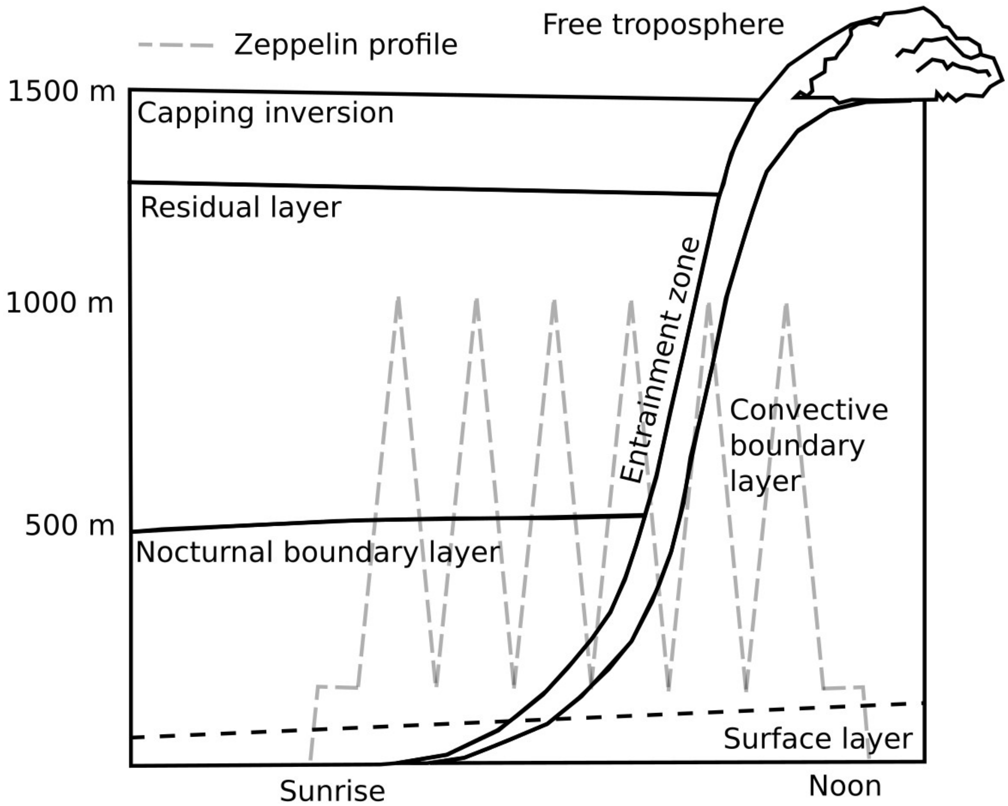

Figure 1: A schematic diagram of different atmospheric layers in the lower troposphere and their development during the morning hours. A generic Zeppelin measurement profile (dashed gray line) is displayed on top. The figure is adapted from Stull (1988)

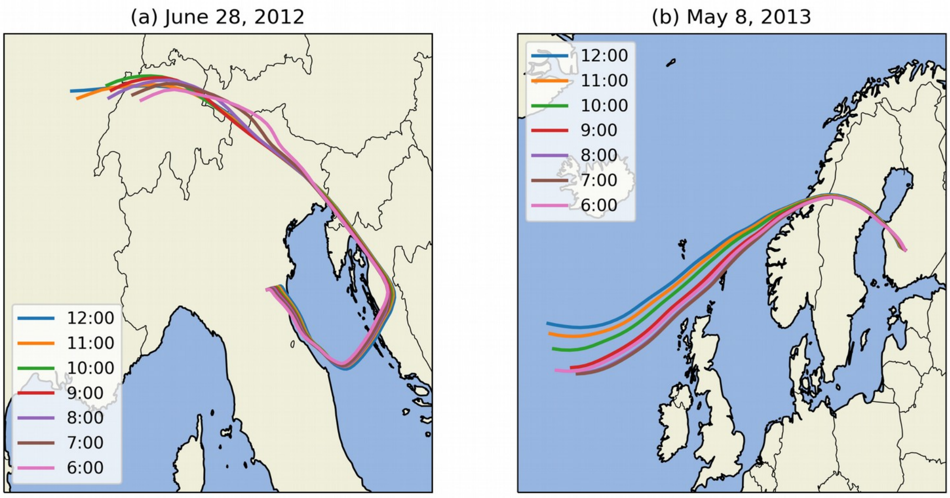

Figure 2: Airmass backward trajectories to (a) SPC during the morning of June 28, 2012 and (b) HTL during the morning of May 8, 2013. The legend shows the hour of airmass arrival in UTC. The arrival altitude was set to 100 m above ground.

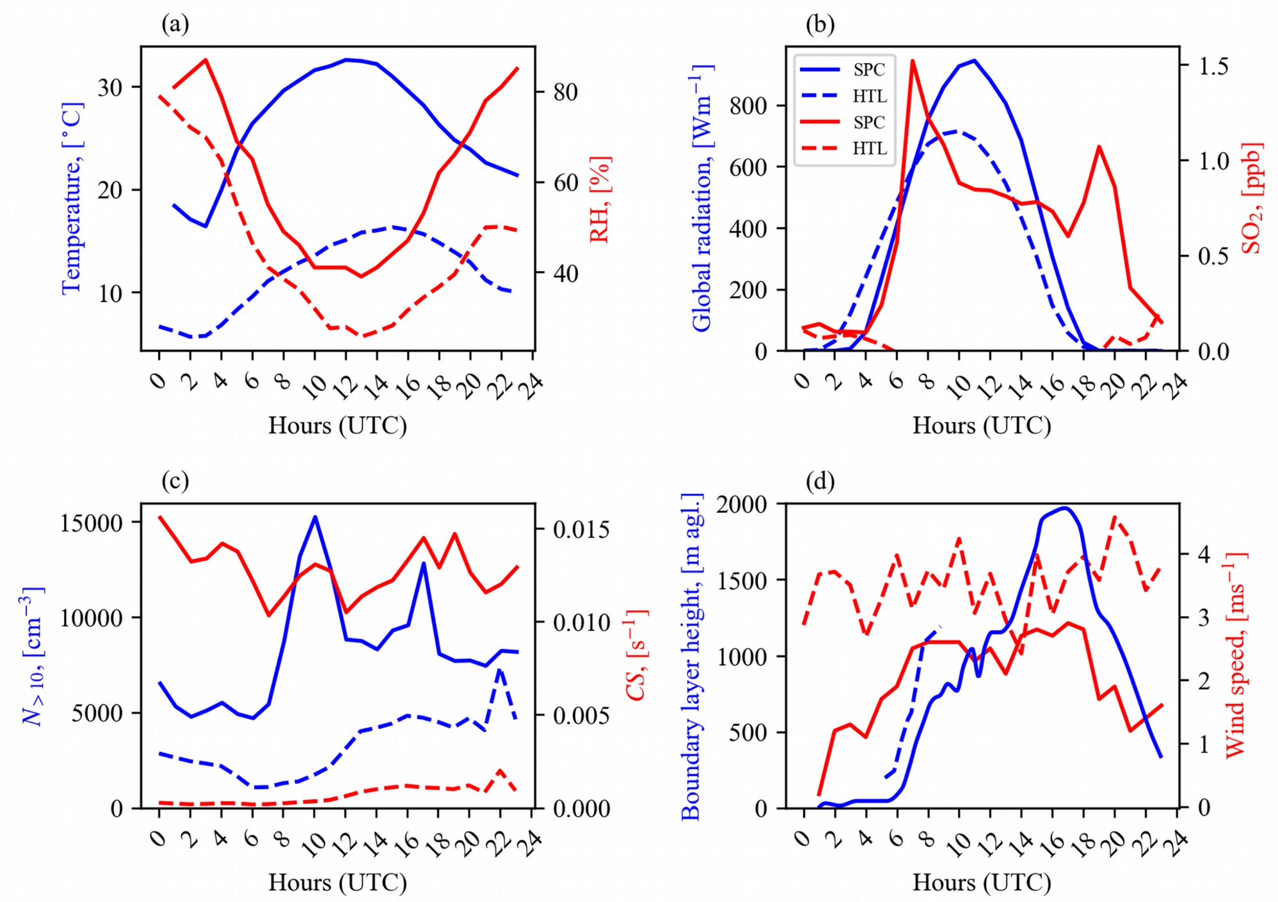

Figure 3: Ground-based measurements of diurnal variation in (a) temperature, relative humidity, (b) global radiation, SO2 concentration, (c) >10 nm particle number concentration, condensation sink (CS) and (d) mixed layer height in SPC on June 28, 2012 and in HTL on May 8, 2013.

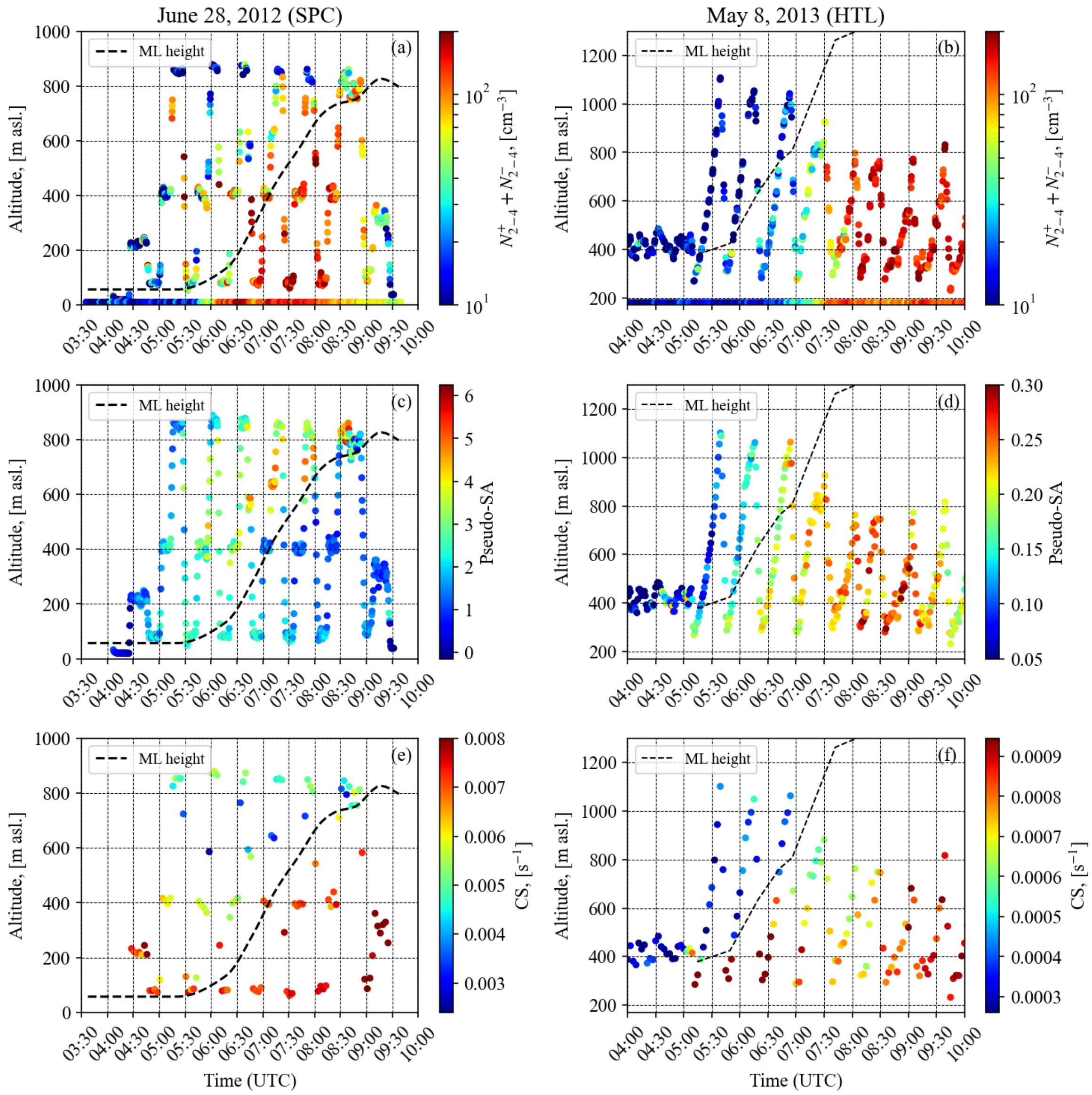

Figure 4: Time-evolution of selected variables as a function of height in SPC on June 28, 2012 and HTL on May 8, 2013. Panels (a) and (b) show the intermediate ion number concentration from SPC and HTL. Ground-based measurements as well as measurements from the Zeppelin are shown. Panels (c) and (d) show the pseudo-SA from SPC and HTL. Panels (e) and (f) show the CS. Height of the mixed layer is shown in all panels.

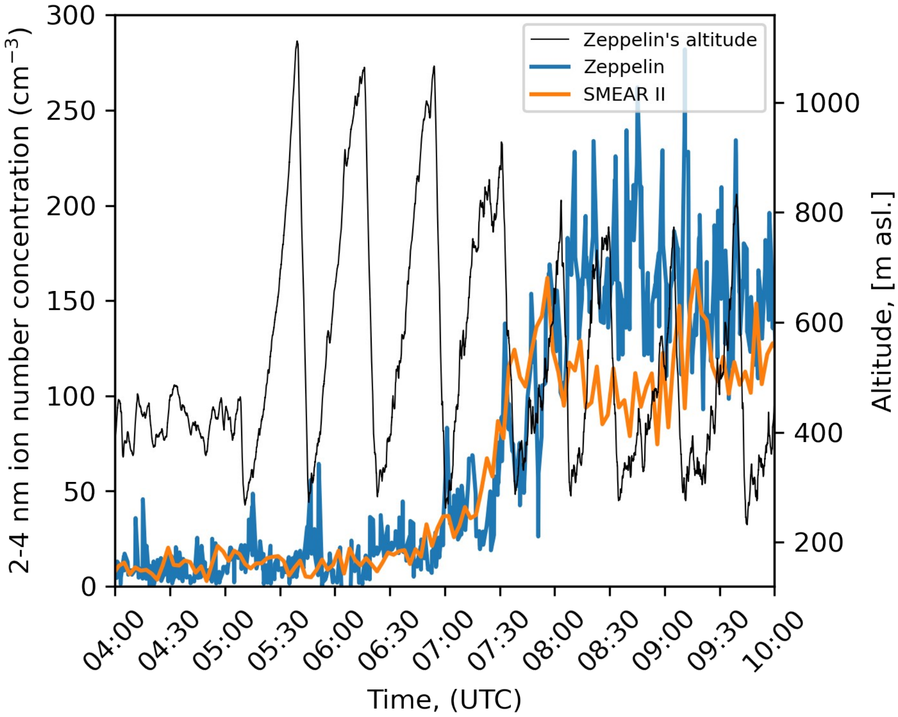

Figure 5: Time series of intermediate (2-4 nm) ion number concentration on board the Zeppelin and the SMEAR II station and the Zeppelin's altitude in HTL on May 8, 2013.

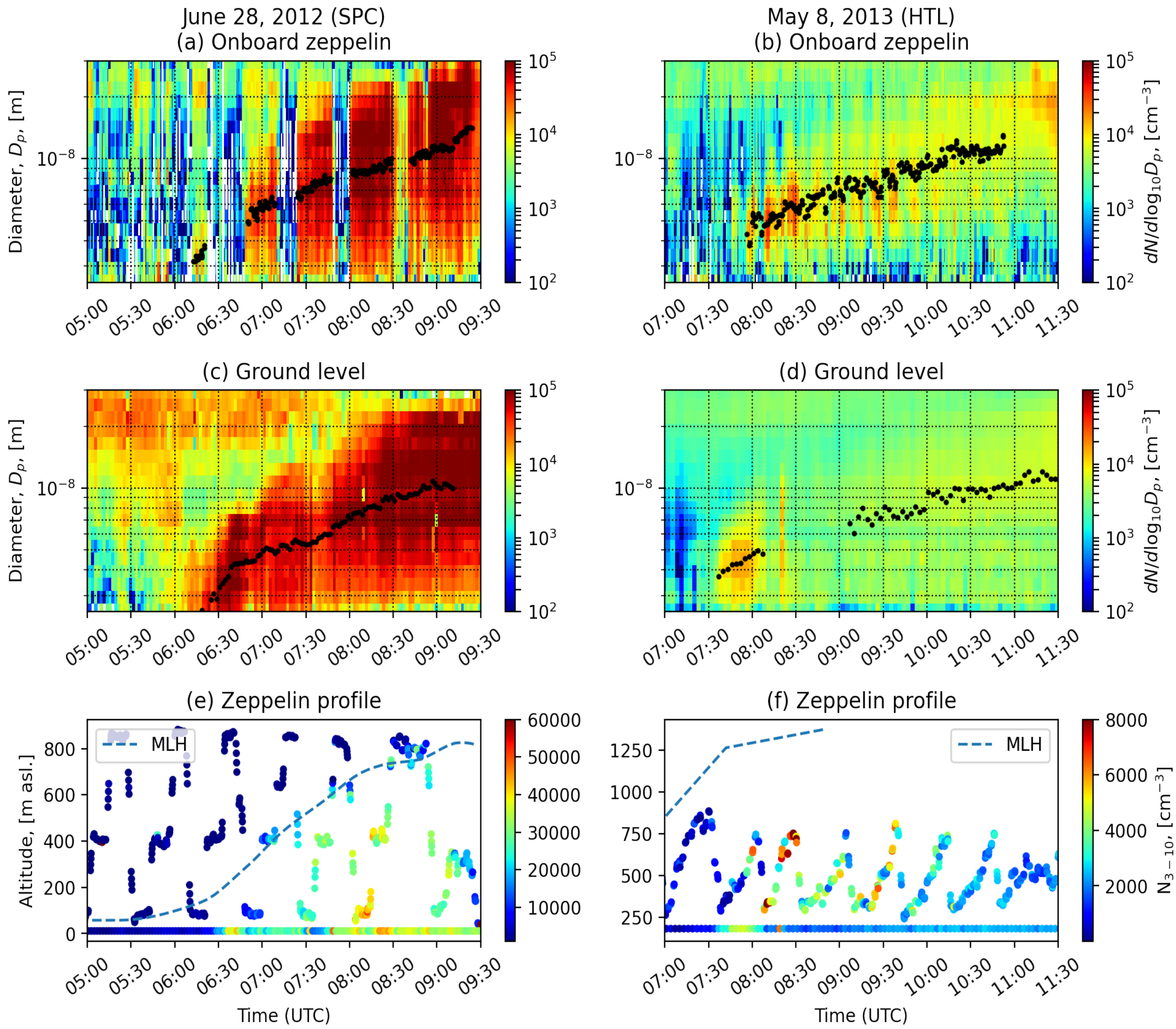

Figure 6: Time evolution of particle number size distributions measured by the NAIS (positive polarity) on board the Zeppelin (a, b) and at the ground level (c, d) in HTL and in SPC on the two case study days. The black dots are the mean mode diameters found by fitting a log-normal distribution over the growing mode. The panels e and f show the 3-10 nm particle number concentration as a function of time and altitude on board the Zeppelin and at the ground-based station. The ML height during the measurement flights is also shown.

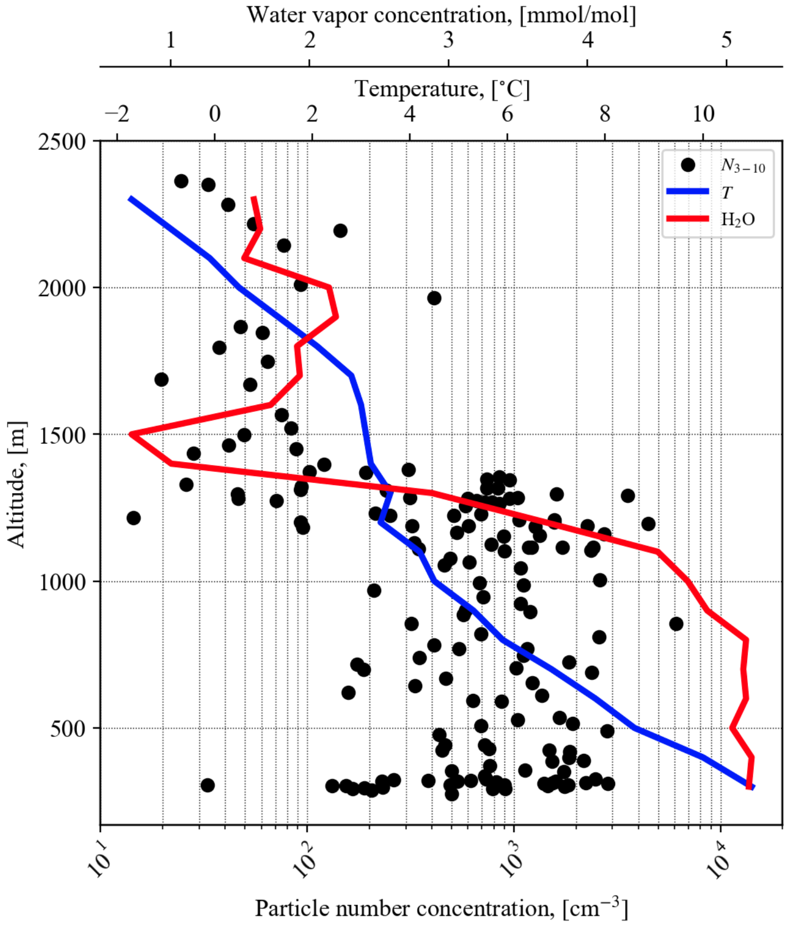

Figure 7: Vertical profile of 3-10 nm particle number concentration (black dots), temperature (blue line) and water vapor concentration (red line) measured on board the Cessna between 07:00-10:00 on May 8, 2013 in HTL.

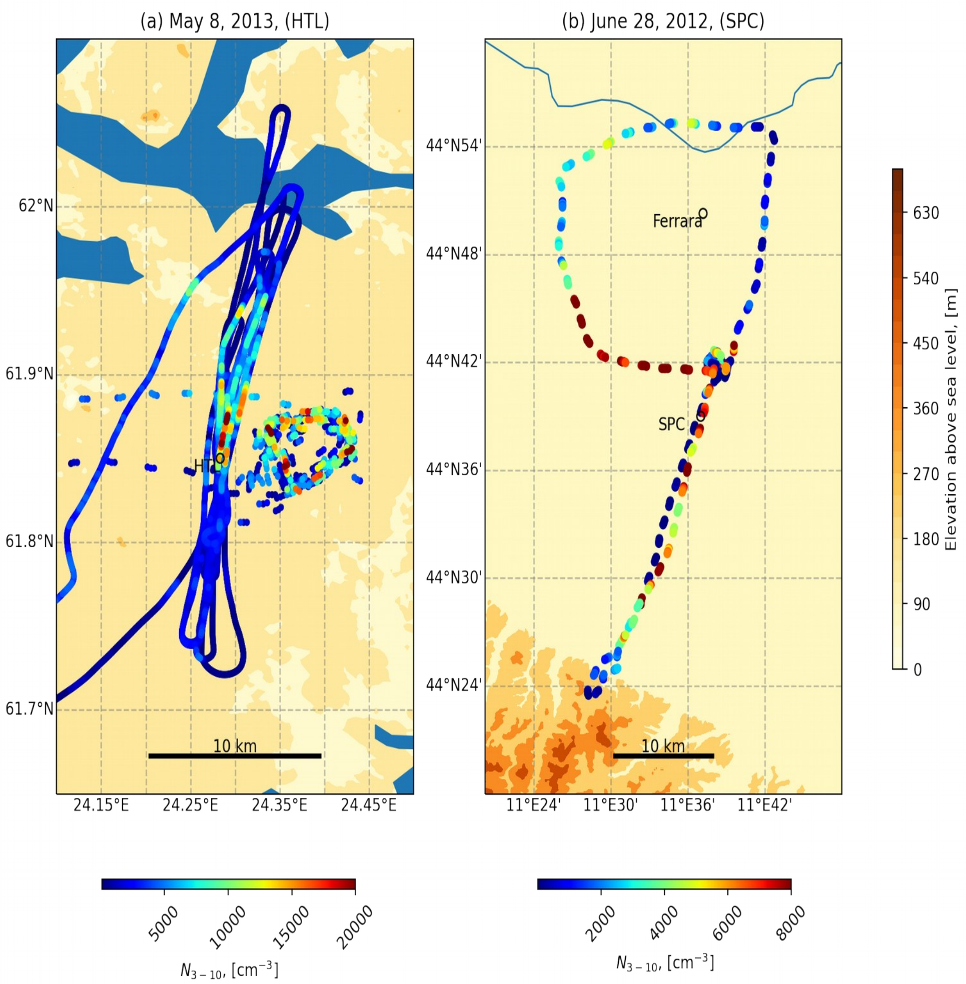

Figure 8: (a) the flight tracks of the Zeppelin (circular track) and the airplane (track with back an forth segments) colored by 3-10 nm particle number concentration from HTL on May 8, 2013. (b) the flight track of the Zeppelin colored by 3-10 nm particle number concentration from SPC on June 30, 2012. The Zeppelin flight track has gaps because the NAIS was measuring in the ion mode during that time.

576

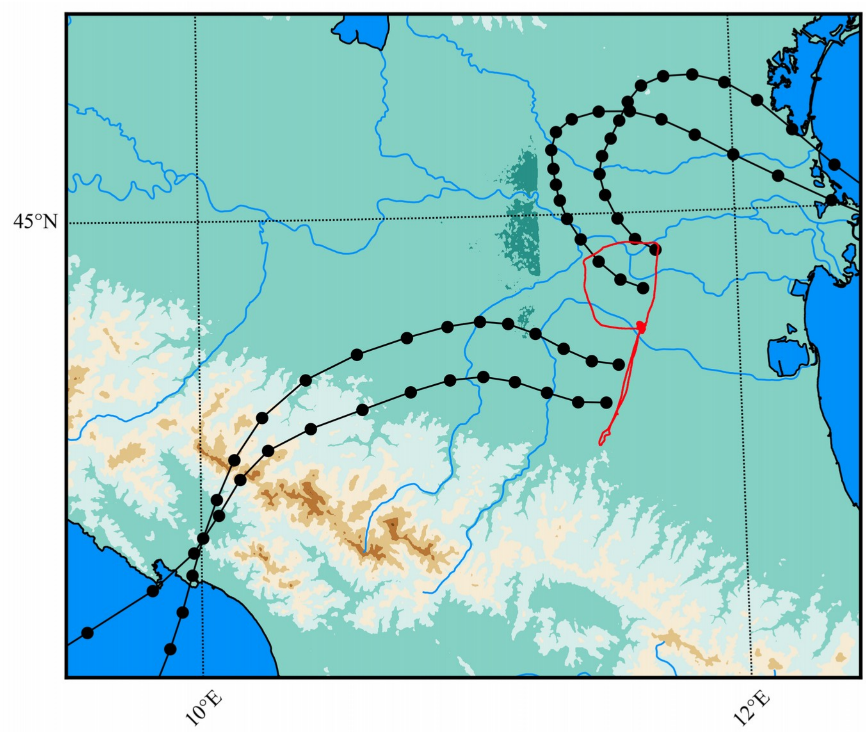

Figure 9: Airmass back trajectories (black dotted lines) arriving to the Zeppelin's measurement area at 8 UTC (when the NPF event started) over north Italy on June 30, 2012. The arrival altitude of the trajectories is 400 m asl. The separation between the dots along the trajectories is one hour. The red line is the Zeppelin's flight track.

Table 1: Calculated particle formation and growth rates. + and – superscripts refer to positive and negative ions respectively. The Zeppelin missed the beginning of the NPF event in SPC and because of that some values are missing.

	HTL (May 8, 2013)		SPC (June 28, 2012)	
	Zeppelin	Ground	Zeppelin	Ground
$J_{1.5}$, [cm^{-3} s^{-1}]	1.5	0.9	-	-
J_3, [cm^{-3} s^{-1}]	0.2	0.3	-	6.8
J_3^-, [cm^{-3} s^{-1}]	0.04	0.04	-	0.04
J_3^+, [cm^{-3} s^{-1}]	0.04	0.04	-	0.03
GR_{1-2}, [nm h^{-1}]	0.8	0.7	-	0.5
GR_{2-3}, [nm h^{-1}]	1.4	1.5	1.8	1.5
GR_{3-7}, [nm h^{-1}]	1.7	1.6	2.9	2.0
GR_{7-20}, [nm h^{-1}]	2.4	2.1	3.0	2.8